Physica A 540 (2020) 123238

Contents lists available at ScienceDirect

Physica A

journal homepage: www.elsevier.com/locate/physa

Resonance phenomena in option pricing with arbitrage

M. Contreras [a,*], J. Echeverría [b], J.P. Peña [a], M. Villena [b]

[a] Universidad Andres Bello, Dpto. de Ciencias Físicas, Sazié 2212, Chile
[b] Faculty of Engineering & Sciences, Universidad Adolfo Ibáñez, Chile

ARTICLE INFO

Article history:
Received 29 August 2018
Received in revised form 7 September 2019
Available online 19 October 2019

Keywords:
Black–Scholes model
Option pricing
Arbitrage
Barrier options

ABSTRACT

In this paper, we want to report an interesting resonance phenomena that appears in option pricing, when the presence of arbitrage is incorporated explicitly into the Black–Scholes model. In Contreras et al. (2010), the authors after analyse empirical financial data, determines that the mispricing between the empirical and the Black–Scholes prices can be described by Heaviside type function (called an arbitrage bubble there). These bubbles are characterised by a finite time span and an amplitude which measures the price deviation from the Black–Scholes model. After that, in Contreras et al. (2010), the Black–Scholes equation is generalised to incorporates explicitly these arbitrage bubbles, which generates an interaction potential that changes the usual Black–Scholes free dynamics completely. However, an interesting phenomena appears when the amplitude of the arbitrage bubble is equal to the volatility parameter of the Black–Scholes model: in that case, the potential becomes infinite, and option pricing decrease abruptly to zero. We analyse this limit behaviour for two situations: a European and a barrier option. Also, we perform an analytic study of the propagator in each case, to understand the cause of the resonance. We think that it resonance phenomena could to help to understand the origin of certain financial crisis in the option pricing area.

1. Introduction

"In order for the light to shine so brightly, the darkness must be present."

[-Francis Bacon, 16th century philosopher-]

Since the original article published by Black and Scholes [1] and Merton [2], the Black–Scholes (B–S) model has evolved and grown into different versions that have generalised the initial assumptions of the model. For example, stochastic volatility models [3–5] and the concept of volatility smile [6–9] incorporate the variability of the volatility parameter in the B–S model. The incorporation of jumps in the base Wiener continuous stochastic process give rise to integro-differential equations [10] for the price of the option. Another evolutionary branch introduces more than one asset, in the so called multi-asset Black–Scholes model [6,11].

A different class of models include the effect of the asset price trajectory: the so called path-dependent options [6]. A special type of path-dependent option is the barrier type of option [12], in which the trajectory effects are generated by imposing boundary conditions on the option price.

* Corresponding author.
E-mail addresses: mauriccio1965@gmail.com, mauric.contreras@uandresbello.edu (M. Contreras), marcelo.villena@uai.cl (M. Villena).

https://doi.org/10.1016/j.physa.2019.123238
0378-4371/

Other different branches of models try to relax the no-arbitrage hypothesis. In fact, economists have realised that in a real market, futures contracts are not always traded at the price predicted by the simple no-arbitrage relation. Strong empirical evidence has supported this point many times and in different settings [13–19].

Most of the attempts to take into account arbitrage in option pricing assume that the return from the B–S portfolio is not equal to the constant risk-free interest rate r_0, changing the no-arbitrage principle to an equation of the form

$$dV(t) = (r_0 + x(t))V(t)\,dt$$

where $x(t)$ is a random arbitrage return. For example, Ilinski [20,21] and Ilinski and Stepanenko [22] assume that $x(t)$ follows an Ornstein–Uhlenbeck process.

Another effort in this direction is Otto [23], who reformulated the original B–S model through a stochastic interest rate. However, as Panayides [24] pointed out, the main problem with this approach is that the random interest rate is not a tradable security, and therefore classical hedging cannot be applied. This difficulty leads to the appearance of an unknown parameter, the market price of risk, which cannot be directly estimated from financial data. Finally, Panayides [24] and Fedotov and Panayides [25] follow an approach suggested by Papanicolaou and Sircar [26], where option pricing with stochastic volatility is modelled. Instead of finding the exact equation for option price, these studies focus on the pricing bands for options that account for random arbitrage opportunities.

In [27] a model of this class was developed, but in which the portfolio return rather than the interest rate follows a stochastic dynamics of the form

$$dV(t) = r_0 V(t) + f(t)V(t)dW,$$

where the amplitude of the Wiener process $f(t)$ is called an arbitrage bubble. In [27] , after analysing empirical financial data, it was shown that the mispricing between the empirical and the Black–Scholes prices can be described by a Heaviside type function in time. This implies that the arbitrage bubble f has the same time dependence. Thus, arbitrage bubbles can be characterised by a finite time span and an height which measures the price deviation from the Black–Scholes model. Note that the arbitrage bubble can be determined from the empirical financial data, as in [28], by using semi-classical methods [29].

From a pure Black–Scholes equation perspective, the presence of the arbitrage bubble produces an interaction potential in the B–S equation which changes completely its usual free dynamics.

In this paper, we use the model developed in [27] to analyse the behaviour of the option price for the case that the bubble amplitude h is close to the volatility parameter. In this situation an interesting phenomenon appears: when the bubble amplitude h is equal to the volatility parameter of the Black–Scholes model, the interaction potential becomes infinite and at the same time, the option pricing decrease abruptly to zero. We analyse this limit behaviour for two situations: European options and barrier options. In the latter case, the resonance is easily visible. Also, we perform an analytic study of the propagator in each case, to understand the cause of the resonance. We think that this resonance phenomenon could help to understand the origin of a certain financial crisis in the option pricing area.

This paper is structured as follows: in Section 2, a summary of the model developed in [27] is given. In Section 3, we analyse the role of the effective interest rate $r(t)$ and study its behaviour for three different bubbles. Section 4 deals with the phenomenon of resonance and its effects on the option price. In Section 5, the properties of the propagator for European options close to the resonance are studied, whereas, in Section 6, the same is done for the barrier options. Section 7 reviews the numerical methods used to integrate the Black–Scholes equation and Sections 8 and 9 presents the results of the numerical integration for European and barrier options, respectively. Finally, Section 10 gives the conclusions of this paper.

2. The black–scholes model with arbitrage

The Black–Scholes model gives the dynamics of the option prices in financial markets. This model has had a long life in finance and has been widely used since the seventies. In its usual arbitrage free version, the B–S equation is given by

$$\frac{\partial \pi}{\partial t} + \frac{\sigma^2}{2} S^2 \frac{\partial^2 \pi}{\partial S^2} + r_0 (S \frac{\partial \pi}{\partial S} - \pi) = 0 \tag{1}$$

where $\pi = \pi(S, t)$ represents the option price as a function of the underlying asset price S and time t.

As is well known, the B–S model for an equity rests on several very restrictive assumptions, such as: (i) the price of the underlying instrument follows a geometric Brownian motion, with constant drift μ and volatility σ (a log-normal random walk), (ii) it is possible to short sell the underlying stock, (iii) there are no dividends on the underlying, (iv) trading in the stock is continuous, in other words, delta hedging is done continuously, (v) there are no transaction costs or taxes, (vi) all securities are perfectly divisible (it is possible to buy any fraction of a share), (vii) it is possible to borrow and lend at a constant risk-free interest rate r_0, and (viii) there are no arbitrage opportunities.

In analytic terms, if $B(t)$ and $S(t)$ are the prices of the risk-free asset and the underlying stock, the price dynamics of the bond and the stock in this model are given by the following equations:

$$\begin{aligned} dB(t) &= r_0 B(t) dt \\ dS(t) &= \alpha S(t) dt + \sigma S(t) dW(t) \end{aligned} \tag{2}$$

where r_0, α and σ are constants and $W(t)$ is a Wiener process.

In order to price the financial derivative, it is assumed that it can be traded, so we can form a portfolio based on the derivative and the underlying stock (no bonds are included). Considering only non dividend paying assets and no consumption portfolios, the purchase of a new portfolio must be financed only by selling from the current portfolio.

Calling $\vec{h}(t) = (h_S, h_\pi)$ the portfolio weights for S and π, $\vec{P}(t) = (S, \pi)$ the price vector of shares and $V(t)$ the value of the portfolio at time t, the dynamics of a self-financing portfolio with no consumption is given by

$$dV(t) = \vec{h}(t)d\vec{P}(t) = h_S dS + h_\pi d\pi \tag{3}$$

In other words, in a model without exogenous incomes or withdrawals, any change of value is due to changes in the asset prices.

Another important assumption for deriving the B–S equation is that the market is efficient in the sense that there are no arbitrage possibilities. This is equivalent to the fact that there exists a self-financed portfolio with value process $V(t)$ satisfying

$$dV(t) = r_0 V(t)dt \tag{4}$$

which means that any locally risk-less portfolio has the same rate of return as the bond.

As mentioned in the introduction, some efforts have been made to relax some of the above assumptions, in particular, the no-arbitrage condition. A model that includes arbitrage possibilities in an explicit way is the gauge field theoretical model developed by Ilinski [20] and Ilinski–Stepanenko [21,22]. Another distinct effort in this direction is Otto [23], who reformulated the original B–S model through a stochastic interest rate. Panayides [24] and Fedotov and Panayides [25] follow an approach suggested by Papanicolaou and Sircar [26], where option pricing with stochastic volatility is modelled.

In [27] there was developed a generalisation of the Black–Scholes model that permits including arbitrage possibilities explicitly, but in an endogenous way. In this model, the usual equation used in the no arbitrage hypothesis is changed to

$$dV(t) = r_0 V(t)dt + f(S,t)V(t)dW(t) \tag{5}$$

where f is any function in (S, t) and W is the same Wiener process driving the random dynamics of the underlying asset price S. The validity of this hypothesis has been tested and validated empirically, see for instance [21].

Now by replacing (3) in (5) one gets

$$h_S dS + h_\pi d\pi = r_0\Big(h_S S + h_\pi \pi\Big)dt + f(S,t)\Big(h_S S + h_\pi \pi\Big)dW(t) \tag{6}$$

where we have used the explicit value of the portfolio $V = h_S S + h_\pi \pi$. By replacing now the Itô law

$$d\pi = \frac{\partial \pi}{\partial t}dt + \frac{\partial \pi}{\partial S}dS + \frac{1}{2}\frac{\partial^2 \pi}{\partial S^2}dS^2 \tag{7}$$

and using (2) for dS one gives

$$\begin{aligned} &h_S\Big(\alpha S dt + \sigma S dW\Big) + h_\pi\left[\left(\frac{\partial \pi}{\partial t} + \alpha S\frac{\partial \pi}{\partial S} + \frac{\sigma^2}{2}S^2\frac{\partial^2 \pi}{\partial S^2}\right)dt + \sigma S\frac{\partial \pi}{\partial S}dW\right] \\ &= r_0\Big(h_S S + h_\pi \pi\Big)dt + f\Big(h_S S + h_\pi \pi\Big)dW \end{aligned}$$

By equating terms in dt and dW of both sides of the above equation, one gets the following system

$$h_S S(\alpha - r_0) + h_\pi\left(\frac{\partial \pi}{\partial t} + \alpha S\frac{\partial \pi}{\partial S} + \frac{\sigma^2}{2}S^2\frac{\partial^2 \pi}{\partial S^2} - r_0\pi\right) = 0 \tag{8}$$

$$h_S S(\sigma - f) + h_\pi\left(\sigma S\frac{\partial \pi}{\partial S} - f\pi\right) = 0 \tag{9}$$

or in matrix form

$$\begin{pmatrix} S(\alpha - r_0) & \left(\frac{\partial \pi}{\partial t} + \alpha S\frac{\partial \pi}{\partial S} + \frac{\sigma^2}{2}S^2\frac{\partial^2 \pi}{\partial S^2} - r_0\pi\right) \\ S(\sigma - f) & \left(\sigma S\frac{\partial \pi}{\partial S} - f\pi\right) \end{pmatrix} \cdot \begin{pmatrix} h_S \\ h_\pi \end{pmatrix} = \begin{pmatrix} 0 \\ 0 \end{pmatrix} \tag{10}$$

These are homogeneous equations for h_S and h_π. In order to obtain non-trivial portfolio the determinant of the above system must be zero. This condition gives the following Black–Scholes equation [27] in the presence of an arbitrage bubble f

$$\frac{\partial \pi}{\partial t} + \frac{\sigma^2}{2}S^2\frac{\partial^2 \pi}{\partial S^2} + \frac{r_0\sigma - \alpha f}{\sigma - f}\left(S\frac{\partial \pi}{\partial S} - \pi\right) = 0 \tag{11}$$

or

$$\frac{\partial \pi}{\partial t}+\frac{\sigma^2}{2}S^2\frac{\partial^2 \pi}{\partial S^2}+(r_0+V(S,t))(S\frac{\partial \pi}{\partial S}-\pi)=0 \tag{12}$$

where

$$V(S,t)=\frac{(r_0-\alpha)f(S,t)}{\sigma-f(S,t)} \tag{13}$$

can be interpreted as an effective potential induced by the arbitrage bubble $f(S,t)$. In this way, the presence of arbitrage generates an external time dependent force, which has an associated potential $V(S,t)$. Then, the incorporation of market imperfections through an arbitrage bubble is equivalent, from a physics point of view, to the problem of a charged particle that interacts with an external electromagnetic field of force. Obviously, when arbitrage disappears, the external potential is zero and we recover the usual B–S dynamics. Thus the B–S model in presence of a arbitrage bubble is a model with interactions and has a different dynamics from the usual free ($f=0$) case. For the interacting model the option price dynamics $\pi(S,t)$ will depend explicitly on the form of the arbitrage bubble $f=f(S,t)$.

From a financial approach, the arbitrage bubbles should have a finite time span and a characteristic amplitude. According to [27], after analysing empirical data for futures, the bubble f can be modelled by a time dependent Heaviside type function of the form

$$f(t)=\begin{cases}0 & 0\leq t\leq T_1\\ h & T_1<t<T_2\\ 0 & T_2\leq tT,\end{cases} \tag{14}$$

so the action of the bubble is restricted to time span $T_1<t<T_2$, and its strength is characterised by its height h. This bubble produces a constant stochastic arbitrage over a finite time interval and then vanishes. It is important to remark that this simple kind of functional form could be used recursively to model almost any case of arbitrage. Note that in [30] an approximate analytical solution for the B–S model, for any form of arbitrage bubble, was obtained. In the present paper we will study the consequences of the simple bubble (14) for the option price dynamics.

The origin of this bubble could be associated to several reasons, such as: transaction costs, asymmetric information issues, short-term volatility, extreme discontinuities, or serial correlations. In our analysis, we are not interested in the causes of all these *market imperfections*. Instead, the important thing for us in this paper is that: (i) once these causes appear, their consequences can be modelled in a simple way through the incorporation of an arbitrage bubble f in the B–S model, and (ii) the effect on the option price dynamics can tested relatively easily.

Thus, any variation of the Black–Scholes dynamics can be associated with an effective bubble, so our model works as a carpet where all the deviations from the usual Black–Scholes theory can be hidden, but these appear then as "bumps" in the carpet, generating then the arbitrage bubbles.

3. The effective interest rate r

From Eqs. (11) and (12) one can see that the net effect of the bubble (14) is to renormalise the constant bare interest rate r_0, by generating an effective variable interest rate $r=r(S,t)$ according to

$$r=r(S,t)=\frac{r_0\sigma-\alpha f(S,t)}{\sigma-f(S,t)}=r_0+V(S,t) \tag{15}$$

This effective interest rate is not directly observable from the finance point of view. It only appears in the interacting B–S model as a consequence of market imperfections. Note that depending on the of the values of the interaction potential, the effective interest rate r can take any value and is not restricted to the interval $0\leq r\leq 1$ as the real financial bare rate r_0 is subject. One can think of r as a free parameter that can take any value and which parametrises the effect of the market's imperfections (through the arbitrage bubble) in the interacting Black–Scholes model. In the absence of markets imperfections no arbitrage appears ($f=0$), so there is no interaction potential at all ($V=0$), and the effective interest rate is the bare financial rate ($r=r_0$). Thus the free dynamical case of our model is just the usual Black–Scholes model. For the interacting case ($V\neq 0$) the effective interest rate r can take any value in principle, and our interacting model goes beyond than the usual Black–Scholes model.

For the particular case of the step bubble (14), r is given by

$$r=r(t)=\begin{cases}r_0 & 0\leq t\leq T_1\\ \bar{r}=\frac{(r_0\sigma-\alpha h)}{(\sigma-h)} & T_1<t<T_2\\ r_0 & T_2\leq t\leq T\end{cases} \tag{16}$$

and the potential V is

$$V=V(t)=\begin{cases}0 & 0\leq t\leq T_1\\ \bar{V}=\frac{(r_0-\alpha)}{(\sigma-h)}h & T_1<t<T_2\\ 0 & T_2\leq t\leq T\end{cases} \tag{17}$$

Table 1
Black–Scholes parameters.

r_0	α	σ	T_1	T_2	T
0.2	0.1	0.3	0.3	0.7	1.0

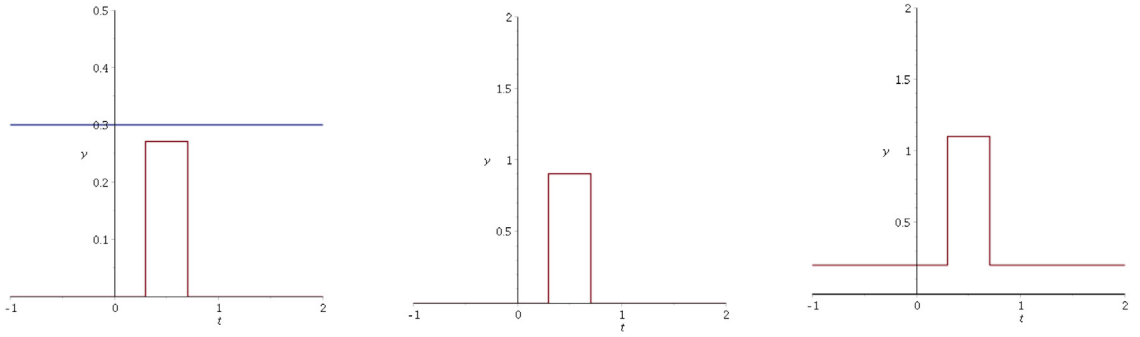

Fig. 1. Step-bubble $f(t)$, potential $V(t)$ and effective interest rate $r(t) = r_0 + V(t)$ for $h = 0.9\sigma$.

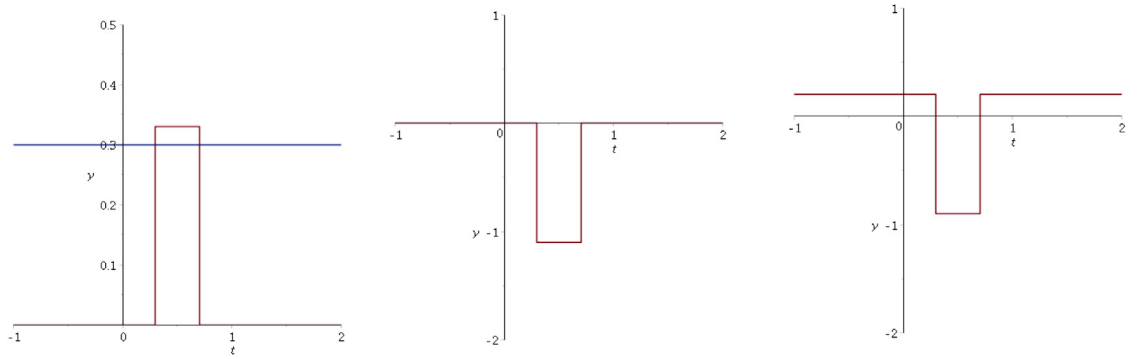

Fig. 2. Step-bubble $f(t)$, potential $V(t)$ and effective interest rate $r(t) = r_0 + V(t)$ for $h = 1.1\sigma$.

Thus, when there is no arbitrage (for $0 \leq t \leq T_1$ or $T_2 \leq t \leq T$), the effective interest rate is just the bare financial rate r_0. But in the interval $T_1 < t < T_2$ when the arbitrage is present, the effective interest rate is

$$r = \bar{r} = \frac{(r_0\sigma - \alpha h)}{(\sigma - h)}$$

and its value can be positive, greater than 1 or even negative, depending on the values of the parameters r_0, α, σ and h.

To see how the effective interest rate r changes with time and what values it can took, Figs. 1 to 6 show (from left to right) the behaviour of the bubble $f(t)$, the potential $V(t)$ and effective interest rate $r(t) = r_0 + V(t)$ respectively, for three different kind of bubbles.

Table 1 shows a set of values for r_0, α, σ, T_1, T_2 and T which will be used in Figs. 1 to 6.

Fig. 1 shows the step-bubble (14) for the case $h = 0.9\sigma$ and Fig. 2 shows the same step-bubble for $h = 1.1\sigma$. The blue line in the left of Figs. 1 and 2 represents the value of the volatility σ. Note that the effective interest rate r becomes negative when the bubble appears for $h = 1.1\sigma$.

Figs. 3 and 4 shows the Lorentz-bubble

$$f(t) = \frac{h}{1 + t^2} \tag{18}$$

Fig. 3 represents the case $h = 0.9\sigma$ and Fig. 4 shows the case $h = 1.1\sigma$. Again blue line in the left of Figs. 3 and 4 represents the value of the volatility σ. Note that the potential and the effective interest rate diverges when the Lorentz-bubble intersect the constant volatility blue line for $h = 1.1\sigma$.

Figs. 5 and 6 shows the Gaussian-bubble

$$f(t) = he^{-\frac{1}{2}t^2} \tag{19}$$

Fig. 5 represents the case $h = 0.9\sigma$ and Fig. 6 shows the case $h = 1.1\sigma$. Again note that the potential and the effective interest rate diverges when the Lorentz-bubble intersect the constant volatility blue line for $h = 1.1\sigma$.

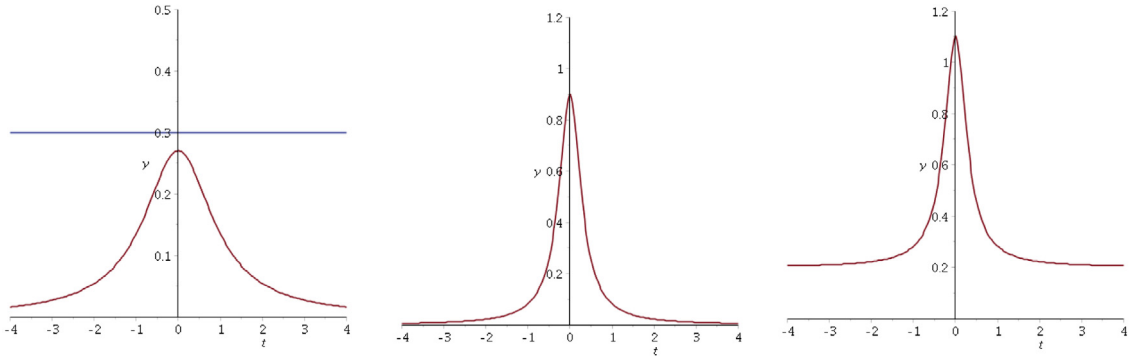

Fig. 3. Bubble $f(t)$, potential $V(t)$ and effective interest rate $r(t) = r_0 + V(t)$ for a Lorentz bubble with maximum height $h = 0.9\sigma$.

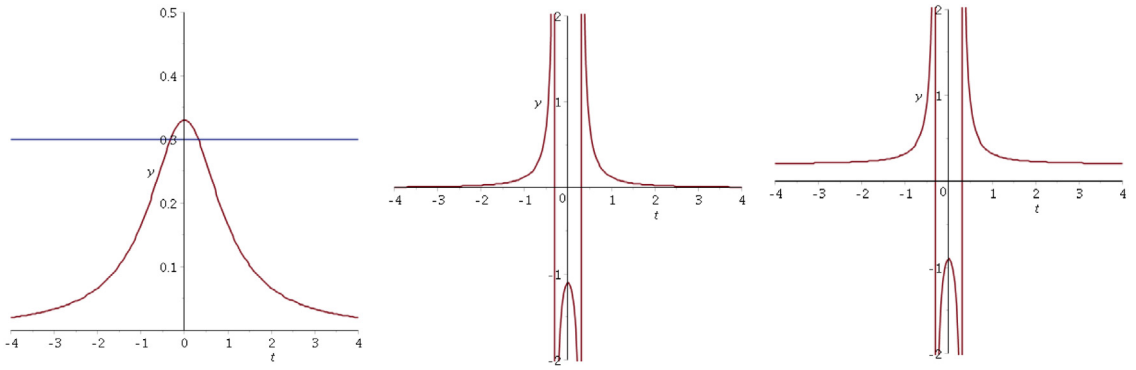

Fig. 4. Bubble $f(t)$, potential $V(t)$ and effective interest rate $r(t) = r_0 + V(t)$ for a Lorentz bubble with maximum height $h = 1.1\sigma$.

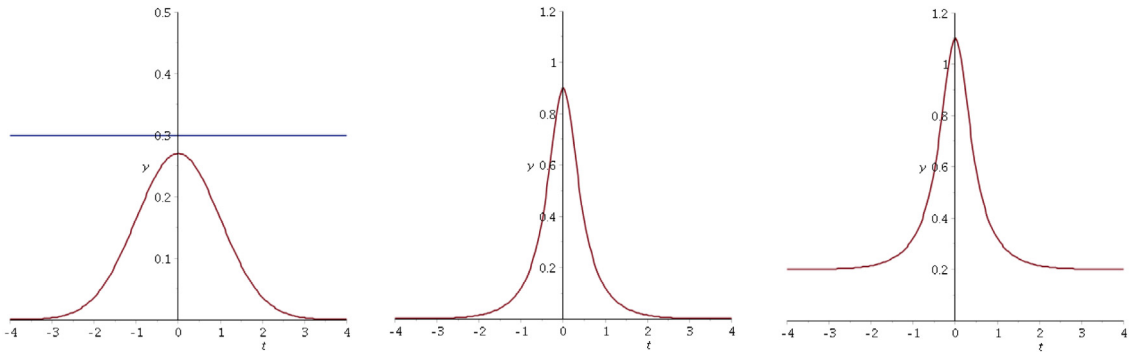

Fig. 5. Gaussian bubble $f(t)$, potential $V(t)$ and effective interest rate $r(t) = r_0 + V(t)$ for a Gaussian bubble with maximum height $h = 0.9\sigma$.

From the above examples, one can see that effective interest rate $r(t)$ in the presence of the arbitrage bubble $f(t)$ can in general take any positive or negative value and is not restricted as the observable financial rate r_0 the sector $0 < r_0 < 1$.

In the rest of the paper, we analyse in detail the effect of the step-bubble (14) over the option price dynamics. This choice is justified by the following several reasons:

(i) The model is mathematically more treatable since it requires determining the propagator of the Black–Scholes equation for a generic constant interest rate, which is widely known in the literature and also has a closed analytical expression. For a Lorentz or Gauss bubble, there is no closed form for propagator, and it must be obtained numerically.

(ii) One can obtain some stylised facts about the behaviour of the interacting option's price in an analytical way and whose conclusions are quite general and can be applied to any other type of bubble.

(iii) Any bubble type can be approximated for a series of step-bubbles, so the knowledge of the option price behaviour for the step-bubble allows to obtain the dynamics of the option in the presence of any bubble.

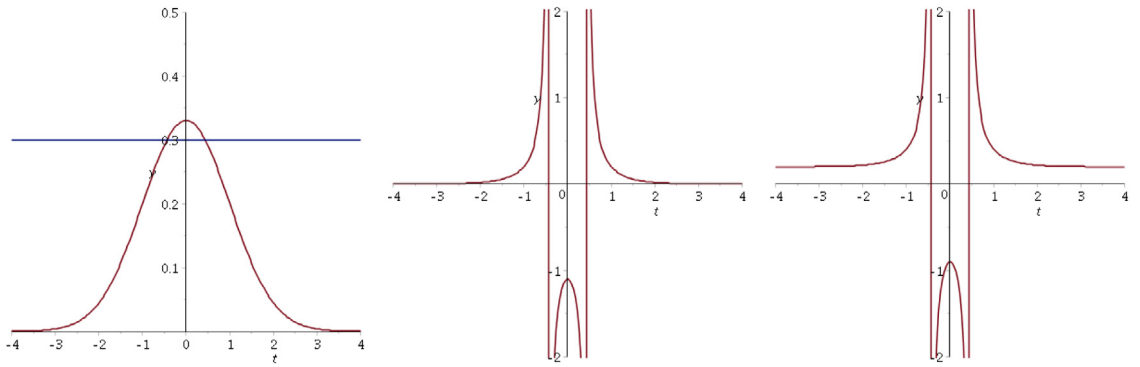

Fig. 6. Gaussian bubble $f(t)$, potential $V(t)$ and effective interest rate $r(t) = r_0 + V(t)$ for a Gaussian bubble with maximum height $h = 1.1\sigma$.

4. The resonance

One interesting special case occurs when the bubble $f(t)$ given in (14) is equal to the volatility σ. In that situation the potential (13) and the effective interest rate (15) becomes infinite. This situation will be called a resonance, in analogy with the usual resonance phenomenon in a mechanical system, when the oscillation amplitude goes to infinite for the resonance frequency. In our case, the effective interest rate r and the interaction potential V goes to infinite at the "resonance value" $f = \sigma$ of the arbitrage bubble.

So one naturally asks: what is the behaviour of the option price at the resonance? What are the implications of the resonance in financial terms?

Clearly, the answer is related to the behaviour of the propagator of the interacting Black–Scholes model.

To study these resonance phenomena we will use the bubble form given in (14). In this case the resonance occurs in the middle interval ($T_1 < t < T_2$) when the height h of the bubble is equal to the volatility σ. In fact, $\bar{r}$ and $\bar{V}$ becomes infinite (see Eqs. (16) and (17)) so

$$r = r(t) = \begin{cases} r_0 & 0 \le t \le T_1 \\ \pm\infty & T_1 < t < T_2 \\ r_0 & T_2 \le t \le T \end{cases} \tag{20}$$

$$V = V(t) = \begin{cases} 0 & 0 \le t \le T_1 \\ \pm\infty & T_1 < t < T_2 \\ 0 & T_2 \le t \le T \end{cases} \tag{21}$$

In the following sections, we analyse the behaviour of the propagator of the interacting B–S model near the resonance for the potential (21) and effective interest rate (20) and we will explore the consequences of this over the option dynamics.

To finish this section, we give a financial interpretation of the resonance. Consider again the Eqs. (8), (9) and (11) or (12). Note that these equations have some interesting limit cases.

The first one is for $\alpha = r_0$, here (8) implies that π satisfies a free Black–Scholes equation for any arbitrage bubble f. Given a solution of π for this free model one can use (9) to obtain the relative hedging h_π/h_S, that is, the number of options shares that can be bought or sold for each unitary share of the underlying stock S. In this case, the relative hedging will depend on the arbitrage bubble, although the option price does not depend on f. In fact the potential in (13) vanishes for this case for any bubble form f.

The second one occurs at the resonance itself. Here (9) implies that for $f = h = \sigma$ in the interval $T_1 \le t \le T_2$, the option price is not given by the usual Black–Scholes equation but instead by

$$S\frac{\partial \pi}{\partial S} - \pi = 0 \tag{22}$$

which implies that

$$\pi = \gamma S \tag{23}$$

with γ a constant. Now replacing this in (8) one obtains

$$h_S(\alpha - r_0)S + h_\pi(\alpha S\gamma - r_0\gamma S) = 0 \tag{24}$$

or

$$\frac{h_\pi}{h_S} = -\gamma \tag{25}$$

Thus, γ must be a negative constant.

Also, one can compare the returns of the asset $S(t)$, the portfolio $V(t)$, and the option price $\pi(t)$. From Eqs. (2), (5) and (7) these returns are

$$\frac{dS}{S} = \alpha\ dt + \sigma dW, \tag{26}$$

$$\frac{dV}{V} = r_0\ dt + f(t)dW, \tag{27}$$

and

$$\frac{d\pi}{\pi} = \frac{1}{\pi}\left(\frac{\partial\pi}{\partial t} + \alpha S\frac{\partial\pi}{\partial S} + \frac{1}{2}\sigma^2 S^2\frac{\partial^2\pi}{\partial S^2}\right)dt + \frac{1}{\pi}\sigma S\frac{\partial\pi}{\partial S}dW, \tag{28}$$

Note that these returns oscillate around of its mean with different amplitudes of the same Brownian motion $W(t)$.

Now, close to the resonance, the potential V in the third term of (12) becomes very large in such way that the Black–Scholes becomes

$$V(S,t)(S\frac{\partial\pi}{\partial S} - \pi) = 0 \tag{29}$$

so one has that at the resonance

$$S\frac{\partial\pi}{\partial S} = \pi. \tag{30}$$

The solution of the last equation is given in (23) Thus, at the resonance

$$\frac{\partial^2\pi}{\partial S^2} = 0, \qquad \frac{\partial\pi}{\partial t} = 0. \tag{31}$$

The return of π at the resonance $f(t) = \sigma$ is then

$$\frac{d\pi}{\pi} = \alpha\ dt + \sigma dW, \tag{32}$$

whereas the returns of S and V at the resonance are

$$\frac{dS}{S} = \alpha\ dt + \sigma dW, \tag{33}$$

$$\frac{dV}{V} = r_0\ dt + \sigma dW, \tag{34}$$

Thus, at the resonance, the stochastic variation of the three returns are the same, and the option price behaves identically to the asset price, that is, they are the same object.

In the following sections, we will analyse the dynamical behaviour of the interacting Black–Scholes model in the time region $T_1 \leq t \leq T_2$ for two different options types: the European and Barrier options and we will obtain its asymptotic characteristic near the resonance $f = h = \sigma$.

5. European options

5.1. The interacting propagator for European options

For the effective interest rate r given by (16) the interacting B–S equation has the same form

$$\frac{\partial\pi}{\partial t} + \frac{\sigma^2}{2}S^2\frac{\partial^2\pi}{\partial S^2} + r(S\frac{\partial\pi}{\partial S} - \pi) = 0 \tag{35}$$

with constant r value for the three temporals regions $I_0 = \{0 \leq t \leq T_1\}$, $I_1 = \{T_1 < t < T_2\}$ and $I_2 = \{T_2 \leq t \leq T\}$. It looks like as a usual free B–S equation, but it is true only in the time intervals I_0 and I_2 where the effective interest rate r is just the real positive financial interest rate r_0.

Instead for the interval I_2, Eq. (35) is an interacting B–S equation, because here $r = \bar{r} = \frac{(r_0\sigma - \alpha h)}{(\sigma - h)}$ which can take any real value and depends on the initial parameters r_0, α, σ and h.

The solution for (35) can be written for a generic constant r value as the convolution

$$\pi(S,t) = \int_0^\infty P(S,S',t,T,r)\,\pi(S',T)\,dS' \tag{36}$$

where

$$P(S,S',t,T,r) = \frac{1}{S'}\frac{e^{-r(T-t)}}{\sqrt{2\pi\sigma^2(T-t)}}e^{-\frac{1}{2\sigma^2(T-t)}[\ln(\frac{S}{S'})+(r-\frac{\sigma^2}{2})(T-t)]^2} \tag{37}$$

is the Black–Scholes propagator, and

$$\pi(S', T) = \Phi(S') \tag{38}$$

is the contract function. Thus the solution of the interacting B–S equation can be written as

$$\pi(S,t) = \begin{cases} \pi_0(S,t) \\ \pi_1(S,t) \\ \pi_2(S,t) \end{cases} = \begin{cases} \int_0^\infty P(S,S',t,T_1,r=r_0)\,\pi_1(S',T_1)\,dS' & 0 \le t \le T_1 \\ \int_0^\infty P(S,S',t,T_2,r=\bar{r})\,\pi_2(S',T_2)\,dS' & T_1 < t < T_2 \\ \int_0^\infty P(S,S',t,T,r=r_0)\,\Phi(S')\,dS' & T_2 < t < T \end{cases} \tag{39}$$

Then, the option price dynamics is completely determined by the propagator $P(S, S', t, T, r)$. In the next section we will analyse the behaviour of this propagator in the time interval I_1 where the resonance appears. That is, we will study $P(S, S', t, T, r)$ for $r = \bar{r} \to \pm\infty$.

5.2. The interacting European propagator near the resonance

To understand the behaviour of the option price near the resonance, we will now study the propagator of the Black–Scholes model (37), which will be written in the form

$$P(S,\tau,r=\bar{r}) = \frac{1}{S'}\frac{e^{-\bar{r}\tau}}{\sqrt{2\pi\sigma^2\tau}} e^{-\frac{1}{2\sigma^2\tau}\phi^2} \tag{40}$$

with

$$\tau = T - t \tag{41}$$

and

$$\phi = \phi(S,t) = \ln(\frac{S}{S'}) + (\bar{r} - \frac{\sigma^2}{2})(T-t) = \ln(\frac{S}{S'}) + (\bar{r} - \frac{\sigma^2}{2})\tau \tag{42}$$

As time passes, the propagator pushes backward the information at the maturity time T (the option contract $\Phi(S)$) back to time $t = 0$. To know the direction in the plane $S - t$ in which this information is propagated, one can follow the trajectory of the maximum of the propagator along the plane $S - t$. The position of this maximum, for each fixed t or τ, is given by the condition

$$\frac{\partial P(S,\tau,\bar{r})}{\partial S} = 0 \tag{43}$$

that is

$$\frac{\partial P(S,\tau,\bar{r})}{\partial S} = -\frac{P(S,\tau,\bar{r})}{\sigma^2\tau S}\phi(S,\tau) = 0 \tag{44}$$

Because we are searching for finite values of S, one has that the maximum S^* is given by the condition

$$\phi(S^*,\tau) = 0$$

or explicitly

$$\ln(\frac{S^*}{S'}) + (\bar{r} - \frac{\sigma^2}{2})\tau = 0 \tag{45}$$

so that

$$S^* = S' e^{-(\bar{r} - \frac{\sigma^2}{2})\tau} \tag{46}$$

and the value of the propagator at the maximum $S = S^*$ is

$$P(S^*,\tau,\bar{r}) = \frac{1}{S'}\frac{e^{-\bar{r}\tau}}{\sqrt{2\pi\sigma^2\tau}} e^{-\frac{1}{2\sigma^2\tau}\phi(S^*)^2} = \frac{1}{S'}\frac{e^{-\bar{r}\tau}}{\sqrt{2\pi\sigma^2\tau}} \tag{47}$$

To study the behaviour of the trajectory maximum's (46) near to the resonance $r = \bar{r} = \pm\infty$ one can evaluate (46) for several interacting $\bar{r}$ values. For example, Figs. 7, 8, 9, and 10 show the trajectory of the maximum (46) of the Black–Scholes propagator in the $S - t$ plane for the cases $r_0 = 0.1$, $\sigma = 0.6$, $S_0 = 5$, $T_1 = 0.4$, $T_2 = 0.6$, $T = 1$ and for $\bar{r} = \pm 1$, $\bar{r} = \pm 10$, $\bar{r} = \pm 30$ and $\bar{r} = \pm 1000$ respectively. Note that the trajectory of the maximum $S^*(t)$ of the propagator (when it goes from the maturity time $T = 1$ to the origin $t = 0$) turns right for greater positive $\bar{r}$ values and, at the same time, its value decreases to zero due to (47). Instead, for greater negative values of $\bar{r}$, $S^*(t)$ turns left at $t = T_2$ and, at the same time, its value increases due to (47).

This behaviour resembles that of light when it goes through a glass. But in this case the direction and behaviour of the "option light ray" depends on the sign of the "refraction index" $\bar{r}$. For the positive case, the "option light ray" is attenuated

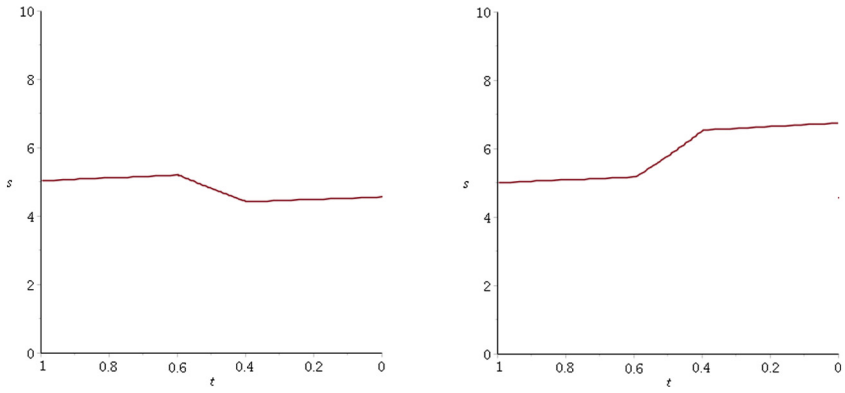

Fig. 7. Behaviour of $S^*(t)$: $\bar{r} = +1$ (left figure) and $\bar{r} = -1$ (right figure).

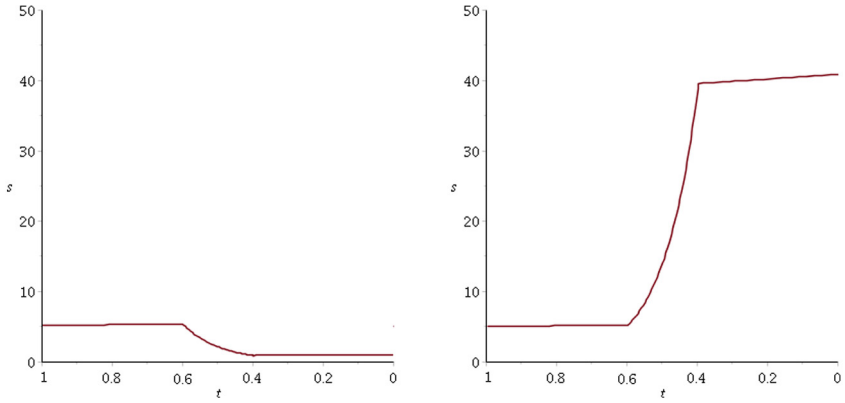

Fig. 8. Behaviour of $S^*(t)$: $\bar{r} = +10$ (left figure) and $\bar{r} = -10$ (right figure).

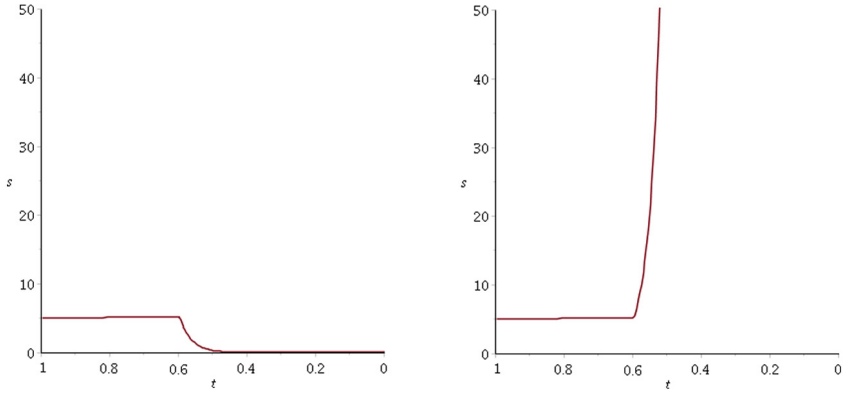

Fig. 9. Behaviour of $S^*(t)$: $\bar{r} = +30$ (left figure) and $\bar{r} = -30$ (right figure).

towards the right, but for the negative case it is amplified towards the left. Thus, the arbitrage bubble can be seen as the effect of a glass over the option propagator's trajectory, and one could analyse its dynamics in terms of a geometric optic framework.

At the resonance, the value of $\bar{r}$ diverges in this case. For $\bar{r} \to \infty$, the "option light ray" at $t = T_2$ turns right and is attenuated instantly. Instead, for $\bar{r} \to -\infty$, the "option light ray" turns left and is amplified to infinity instantly. This is analogous to the phenomenon of total internal reflection in optics.

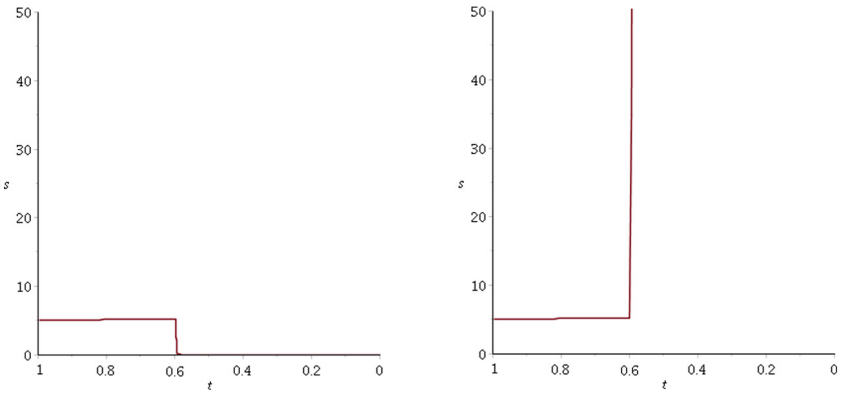

Fig. 10. Behaviour of $S^*(t)$: $\bar{r} = +1000$ (left figure) and $\bar{r} = -1000$ (right figure).

6. Barrier options

6.1. The interacting propagator for barrier options

For a barrier option, the solution of the B–S equation for a generic constant r value is [6,12]

$$\pi(S,t) = \int_0^\infty P_B(S,S',t,T,r)\,\pi(S',T)\,dS' \tag{48}$$

where

$$P_B = P(S,S',t,T,r) - \left(\frac{B}{S}\right)^{\left(\frac{2r}{\sigma^2}-1\right)} P(\frac{B^2}{S},S',t,T,r) \tag{49}$$

is the propagator for the barrier option, $P(S,S',t,T,r)$ is the Black–Scholes propagator (37) and $\pi(S',T) = \Phi(S')$ is the contract function. For the case of the bubble (14) the solution of the barrier option is

$$\pi_B(S,t) = \begin{cases} \pi_{B0}(S,t) \\ \pi_{B1}(S,t) \\ \pi_{B2}(S,t) \end{cases} = \begin{cases} \int_0^\infty P_B(S,S',t,T_1,r=r_0)\,\pi_{B1}(S',T_1)\,dS' & 0 \le t \le T_1 \\ \int_0^\infty P_B(S,S',t,T_2,r=\bar{r})\,\pi_{B2}(S',T_2)\,dS' & T_1 < t < T_2 \\ \int_0^\infty P_B(S,S',t,T,r=r_0)\,\Phi(S')\,dS' & T_2 < t < T. \end{cases} \tag{50}$$

Again, the barrier option dynamics is completely determined by the barrier propagator. We now study the behaviour of the barrier propagator in the time region $T_1 < t < T_2$ for $r = \bar{r} \to \pm\infty$

6.2. The interacting barrier propagator near the resonance

We will write the barrier propagator for short as

$$P_B(S,\tau,r=\bar{r}) = P(S,\tau,\bar{r}) - \left(\frac{B}{S}\right)^{\left(\frac{2\bar{r}}{\sigma^2}-1\right)} P(\frac{B^2}{S},\tau,\bar{r}) \tag{51}$$

In this case, for each fixed t or τ, the maximum of the barrier option is given by the condition

$$\frac{\partial P_B(S,\tau,\bar{r})}{\partial S} = 0 \tag{52}$$

that is

$$\frac{\partial P(S,\tau,\bar{r})}{\partial S} + \frac{(\frac{2\bar{r}}{\sigma^2}-1)}{S}\left(\frac{B}{S}\right)^{\left(\frac{2\bar{r}}{\sigma^2}-1\right)} P(\frac{B^2}{S},\tau,\bar{r}) - \left(\frac{B}{S}\right)^{\left(\frac{2\bar{r}}{\sigma^2}-1\right)} \frac{\partial P(\frac{B^2}{S},\tau,\bar{r})}{\partial S} = 0 \tag{53}$$

Now

$$\frac{\partial P(S,\tau,\bar{r})}{\partial S} = -P(S,\tau,\bar{r})\left[\frac{\ln(\frac{S}{S'}) + (\bar{r} - \frac{\sigma^2}{2})(T-t)}{\sigma^2\tau S}\right] \tag{54}$$

$$\frac{\partial P(\frac{B^2}{S},\tau,\bar{r})}{\partial S} = P(\frac{B^2}{S},\tau,\bar{r})\left[\frac{\ln(\frac{B^2}{SS'}) + (\bar{r} - \frac{\sigma^2}{2})(T-t)}{\sigma^2\tau S}\right] \tag{55}$$

so we have then

$$P(S,\tau,\bar{r})\left[\frac{\ln(\frac{S}{S'})+(\bar{r}-\frac{\sigma^2}{2})\tau}{\sigma^2\tau S}\right]=P(\frac{B^2}{S},\tau,\bar{r})\left(\frac{B}{S}\right)^{\left(\frac{2\bar{r}}{\sigma^2}-1\right)}\left(\frac{(\frac{2\bar{r}}{\sigma^2}-1)}{S}-\left[\frac{\ln(\frac{B^2}{SS'})+(\bar{r}-\frac{\sigma^2}{2})\tau}{\sigma^2\tau S}\right]\right) \tag{56}$$

or

$$-P(S,\tau,\bar{r})[\ln(\frac{S}{S'})+(\bar{r}-\frac{\sigma^2}{2})\tau]=P(\frac{B^2}{S},\tau,\bar{r})\left(\frac{B}{S}\right)^{\left(\frac{2\bar{r}}{\sigma^2}-1\right)}[\ln(\frac{B^2}{SS'})-(\bar{r}-\frac{\sigma^2}{2})\tau] \tag{57}$$

By replacing $P(S,\tau,\bar{r})$ and $P(\frac{B^2}{S},\tau,\bar{r})$ using (37) which have the same common factor $\frac{1}{S'}\frac{e^{-\bar{r}\tau}}{\sqrt{2\pi\sigma^2\tau}}$, which can be simplified, one obtains

$$-e^{\frac{-\phi^2}{2\sigma^2\tau}}\phi=\left(\frac{B}{S}\right)^{\left(\frac{2\bar{r}}{\sigma^2}-1\right)}e^{\frac{-\tilde{\phi}^2}{2\sigma^2\tau}}\tilde{\phi}^* \tag{58}$$

where

$$\tilde{\phi}=\ln(\frac{B^2}{SS'})+(\bar{r}-\frac{\sigma^2}{2})\tau \tag{59}$$

$$\tilde{\phi}^*=\ln(\frac{B^2}{SS'})-(\bar{r}-\frac{\sigma^2}{2})\tau \tag{60}$$

and ϕ is defined by Eq. (42).

It is not possible to find, from Eq. (58), an explicit expression for $S=S^*(t)$ or $S=S^*(\tau)$. So, instead, we will try to solve for it implicitly. Thus, we assume there exist a solution $S=S^*(\tau)$ and its inverse $\tau=\tau(S)$. Let

$$f(S,\tau)=e^{\frac{-\phi^2}{2\sigma^2\tau}}\phi+\left(\frac{B}{S}\right)^{\left(\frac{2\bar{r}}{\sigma^2}-1\right)}e^{\frac{-\tilde{\phi}^2}{2\sigma^2\tau}}\tilde{\phi}^*=0. \tag{61}$$

Now by taking the derivative with respect to S along the curve $\tau=\tau(S)$, the above equation yields

$$\frac{df(S,\tau(S))}{dS}=\frac{\partial f}{\partial S}+\frac{\partial f}{\partial\tau}\frac{d\tau(S)}{dS}=0 \tag{62}$$

so one can obtain $\tau'(S)=\frac{d\tau(S)}{dS}$ as

$$\tau'(S)=-\frac{\left(\frac{\partial f}{\partial S}\right)}{\left(\frac{\partial f}{\partial\tau}\right)} \tag{63}$$

or

$$\tau'=\frac{\frac{1}{S}\left[\left(\frac{B}{S}\right)^{\left(\frac{2\bar{r}}{\sigma^2}-1\right)}e^{\frac{-\tilde{\phi}^2}{2\sigma^2\tau}}\left(\frac{\tilde{\phi}^*\tilde{\phi}}{\sigma^2\tau}-\tilde{\phi}^*(\frac{2\bar{r}}{\sigma^2}-1)-1\right)-e^{\frac{-\phi^2}{2\sigma^2\tau}}\left(\frac{\phi^2}{\sigma^2\tau}-1\right)\right]}{-e^{\frac{-\phi^2}{2\sigma^2\tau}}\left(\phi\left(\frac{\phi^2}{2\sigma^2\tau^2}-\frac{\phi(\bar{r}-\frac{\sigma^2}{2})}{\sigma^2\tau}\right)+\bar{r}-\frac{\sigma^2}{2}\right)-\left(\frac{B}{S}\right)^{\left(\frac{2\bar{r}}{\sigma^2}-1\right)}e^{\frac{-\tilde{\phi}^2}{2\sigma^2\tau}}\left(\frac{\sigma^2}{2}-\bar{r}+\tilde{\phi}^*\left(\frac{\tilde{\phi}^2}{2\sigma^2\tau^2}-\frac{\tilde{\phi}(\bar{r}-\frac{\sigma^2}{2})}{\sigma^2\tau}\right)\right)} \tag{64}$$

This is a very complicated expression, but we only need to evaluate it near of the resonance, that is, in the limit $\bar{r}\to\pm\infty$. In this limit, one has that

$$\phi\to\bar{r}\tau$$

$$\tilde{\phi}\to\bar{r}\tau$$

$$\tilde{\phi}^*\to-\bar{r}\tau$$

So, in this limit,

$$\tau'(S)\approx\frac{1}{S}\frac{\left(\frac{B}{S}\right)^{\left(\frac{2\bar{r}}{\sigma^2}-1\right)}\left(\frac{\bar{r}^2\tau}{\sigma^2}-\bar{r}\tau-1\right)-\frac{\bar{r}^2\tau}{\sigma^2}+1}{\left(\bar{r}+\frac{\bar{r}^2\tau}{2}-\frac{\bar{r}^3\tau}{2\sigma^2}-\frac{\sigma^2}{2}\right)\left(\left(\frac{B}{S}\right)^{\left(\frac{2\bar{r}}{\sigma^2}-1\right)}-1\right)}. \tag{65}$$

Consider first the limit $\bar{r}\to\infty$. For $B>S$ by conserving only the largest powers, we have

$$\tau'(S)\approx\frac{1}{S}\frac{\frac{\bar{r}^2\tau}{\sigma^2}\left(\left(\frac{B}{S}\right)^{\left(\frac{2\bar{r}}{\sigma^2}-1\right)}-1\right)}{-\frac{\bar{r}^3\tau}{2\sigma^2}\left(\left(\frac{B}{S}\right)^{\left(\frac{2\bar{r}}{\sigma^2}-1\right)}-1\right)}=-\frac{2}{S\bar{r}} \tag{66}$$

For $B < S$ we have

$$\tau'(S) \approx \frac{1}{S} \frac{-\frac{\bar{r}^2\tau}{\sigma^2}}{\left(-\frac{\bar{r}^3\tau}{2\sigma^2}\right)(-1)} = -\frac{2}{S\bar{r}} \tag{67}$$

For the limit $\bar{r} \to -\infty$, the above expression for $B > S$ goes to

$$\tau'(S) \approx \frac{1}{S} \frac{-\frac{\bar{r}^2\tau}{\sigma^2}}{\left(-\frac{\bar{r}^3\tau}{2\sigma^2}\right)(-1)} = -\frac{2}{S\bar{r}} \tag{68}$$

and for $B < S$

$$\tau'(S) \approx \frac{1}{S} \frac{\frac{\bar{r}^2\tau}{\sigma^2}\left(\left(\frac{B}{S}\right)^{\left(\frac{2\bar{r}}{\sigma^2}-1\right)} - 1\right)}{-\frac{\bar{r}^3\tau}{2\sigma^2}\left(\left(\frac{B}{S}\right)^{\left(\frac{2\bar{r}}{\sigma^2}-1\right)} - 1\right)} = -\frac{2}{S\bar{r}} \tag{69}$$

Thus, whereas be the case, we have the asymptotic expression for $\tau'(S)$ in the limit $\bar{r} \to \pm\infty$

$$\frac{d\tau(S)}{dS} \approx -\frac{2}{S\bar{r}} \tag{70}$$

Hence, at the resonance, one has exactly that

$$\frac{d\tau(S)}{dS} = 0 \tag{71}$$

which is equivalent to saying that the inverse relation for $\bar{r} \to \pm\infty$ satisfies

$$\frac{dS(\tau)}{d\tau} = \mp\infty \tag{72}$$

Thus, when the propagator reaches the "bubble glass" at $t = T_2$, for $\bar{r} \to +\infty$ it turn left and for $\bar{r} \to -\infty$ it turn right.

Now the asymptotic equation (70) can be written for $S(\tau)$ as

$$\frac{dS(\tau)}{d\tau} \approx -\frac{\bar{r}S}{2} \tag{73}$$

The solution of the last equation gives the trajectory of the barrier propagator maximum for the limit of greater $|\bar{r}|$ values, so

$$S^*(\tau) \approx S' e^{-\frac{\bar{r}\tau}{2}} \qquad |\bar{r}| \gg 1. \tag{74}$$

By using this last expression, one can find the time dependence of all functions for $|\bar{r}| \gg 1$, for example,

$$\phi(S^*(\tau)) \approx -\frac{\bar{r}\tau}{2} + \bar{r}\tau = \frac{\bar{r}\tau}{2} \tag{75}$$

$$\tilde{\phi}(S^*(\tau)) \approx -\frac{B^2}{S'^2}\frac{\bar{r}\tau}{2} + \bar{r}\tau = \bar{r}\tau\left(1 - \frac{B^2}{2S'^2}\right). \tag{76}$$

$$\tilde{\phi}^*(S^*(\tau)) \approx -\frac{B^2}{S'^2}\frac{\bar{r}\tau}{2} - \bar{r}\tau = -\bar{r}\tau\left(1 + \frac{B^2}{2S'^2}\right). \tag{77}$$

So, for $|\bar{r}| \gg 1$, the barrier propagator (51) behaves according to

$$P_B(S,\tau,\bar{r}) \approx \frac{1}{S'}\frac{e^{-\bar{r}\tau}}{\sqrt{2\pi\sigma^2\tau}}\left(e^{-\frac{\left[\frac{\bar{r}\tau}{2}\right]^2}{2\sigma^2\tau}} - \left(\frac{B}{S}\right)^{\left(\frac{2\bar{r}}{\sigma^2}-1\right)} e^{-\frac{\left[\bar{r}\tau\left(1-\frac{B^2}{2S'^2}\right)\right]^2}{2\sigma^2\tau}}\right) \tag{78}$$

or

$$P_B(S,\tau,\bar{r}) \approx \frac{1}{S'}\frac{e^{-\bar{r}\tau}}{\sqrt{2\pi\sigma^2\tau}}\left(e^{-\frac{\bar{r}^2\tau}{8\sigma^2}} - \left(\frac{B}{S}\right)^{\left(\frac{2\bar{r}}{\sigma^2}-1\right)} e^{-\frac{\bar{r}^2\tau\left(1-\frac{B^2}{2S'^2}\right)^2}{2\sigma^2}}\right) \tag{79}$$

Note that in this case, the barrier propagator $P_B(S,\tau,\bar{r})$ decreases to zero for both $\bar{r} \to \infty$ and $\bar{r} \to -\infty$.

Thus, the barrier propagator, once it reaches the "bubble glass" at $t = T_2$, coming from $t = T$, turns right (for $\bar{r} \gg 1$) or left (for $\bar{r} \ll -1$) and at the same time it decreases to zero in both directions. At the resonance, this happens instantly, so an observer situated behind the "bubble glass" at $t = T_1$ will never see the "option light ray." Then, the price of the barrier option at the resonance would always go to zero.

7. Numerical simulation

After the analytical analysis performed above, we also compute the option prices by solving the Black–Scholes equation in the presence of an arbitrage bubble (12) numerically. We use an explicit finite-difference method for parabolic partial differential equations.

We construct a grid in the underlying price–time space rectangle $[0, B] \times [0, T]$ by defining a time step Δt and an asset step ΔS, both constant. Thus the grid is made up of the points at the asset values $S_i = i\Delta S$ and times $t_k = T - k\Delta t$, where $0 \leq i \leq I$ and $0 \leq k \leq K$. If π_i^k defines the option value at the point (i, k), use central differences for the S-derivatives and suppose that we choose an asset step size such as the barrier B is a grid point, that is, $B = I\Delta S$.

The finite difference version of Eq. (12) then becomes:

$$\frac{\pi_i^k - \pi_i^{k+1}}{\Delta t} + a_i^k \frac{\pi_{i+1}^k - 2\pi_i^k + \pi_{i-1}^k}{\Delta S^2} + b_i^k \frac{\pi_{i+1}^k - \pi_{i-1}^k}{2\Delta S} + c_i^k \pi_i^k = O(\Delta t, \Delta S^2) \tag{80}$$

where a_i^k, b_i^k and c_i^k are the discrete forms of the coefficients of the equation evaluated at the points of the grid. By rearranging some terms, we can get the recurrence equation

$$\pi_i^{k+1} = A_i^k \pi_{i-1}^k + B_i^k \pi_i^k + C_i^k \pi_{i+1}^k \tag{81}$$

with

$$A_i^k = \nu_1 a_i^k - \frac{1}{2}\nu_2 b_i^k, \tag{82}$$

$$B_i^k = 1 - 2\nu_1 a_i^k + \Delta t c_i^k, \tag{83}$$

$$C_i^k = \nu_1 a_i^k + \frac{1}{2}\nu_2 b_i^k \tag{84}$$

$$\nu_1 = \frac{\Delta t}{\Delta S^2} \quad \text{and} \quad \nu_2 = \frac{\Delta t}{\Delta S} \tag{85}$$

which holds for interior points, i.e. $i = 1, \ldots, I - 1$, giving $I - 1$ equations for the $I + 1$ unknowns. The remaining two equations come from the boundary conditions at $i = 0$ and $i = I$.

8. Results for European options

8.1. European call options

Fig. 11 shows the results of the numerical integration of the B–S equation (11) under the action of the arbitrage bubble (14) in the case of a European call option $\Phi(S) = \max\{0, S - K\}$ for several quotients $\frac{h}{\sigma}$ as indicated in Fig. 11. Here, $r_0 = 0.2, \alpha = 0.1, \sigma = 0.3, T_1 = 0.3, T_2 = 0.7, T = 1$ and $K = 1$. Note that near the resonance but with $h < \sigma$, the effective interest rate $\bar{r}$ is positive, so the propagator turns right, dragging the boundary information at $S = 2$ in that direction. For $h > \sigma$, $\bar{r}$ is negative, so the propagator turns left, in this case dragging the boundary condition $\pi(S = 0, 0) = 0$ at $S = 0$ to the left. The net result is that the option value decreases at $t = 0$ for this last situation near the resonance.

8.2. European binary options

Fig. 12 shows the results of the numerical integration of the B–S equation (11) in the case of a European binary option

$$\Phi(S) = \begin{cases} 0 & 0 \leq S \leq K \\ 1 & S > K \end{cases}$$

for several quotients $\frac{h}{\sigma}$. We use the same parameter values as in Fig. 11. Note that near the resonance but with $h < \sigma$, the propagator turn right dragging the boundary information at $S = 2$ in that direction. For $h > \sigma$, the propagator turn left dragging in this case the boundary condition $\pi(S = 0, 0) = 0$ at $S = 0$ to the left. The net result, again, is that the option value decreases at $t = 0$ near the resonance for this last situation.

9. Results for barrier options

9.1. Barrier call options

Fig. 13 shows the results of the numerical integration of the B–S equation (11) under the action of the arbitrage bubble (14) in the case of a barrier call option for several quotients $\frac{h}{\sigma}$ as indicated in Fig. 13. The parameters used are the same as in Fig. 11. Note that near the resonance but with $h < \sigma$, the propagator turns right and the same time decreases its value. For $h > \sigma$, the propagator turns left dragging information of the middle sector of the option to the left. Now, the

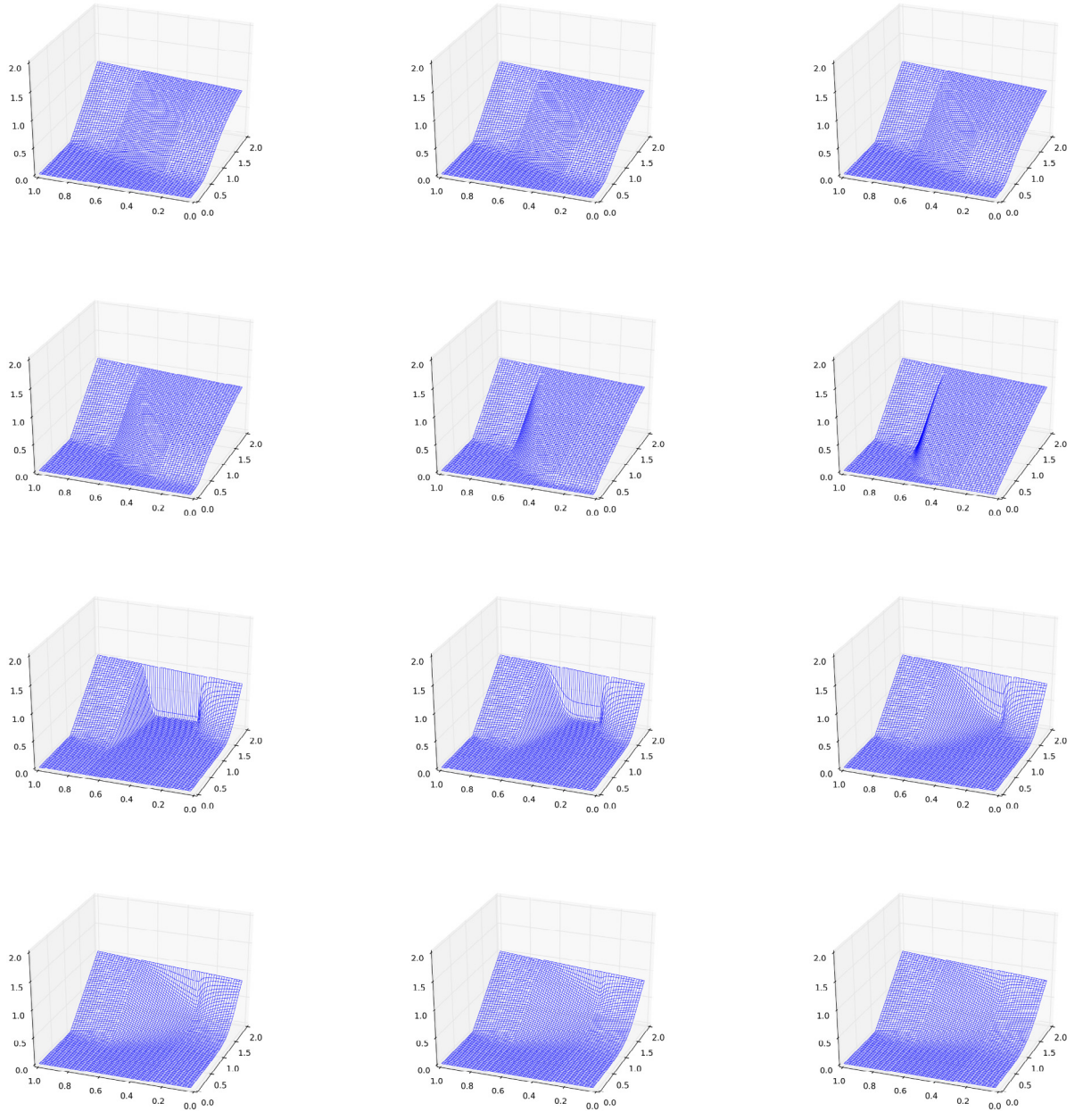

Fig. 11. From left to right and from top to bottom, European call options for $\frac{h}{\sigma}$ = 0.90, 0.92, 0.94, 0.96, 0.98, 0.99, 1.01, 1.02, 1.04, 1.06, 1.08, 1.10 respectively.

net result is that the option value at time $t = 0$, decreases to zero very near the resonance for both the left and right directions.

Fig. 14 shows the behaviour of the barrier call option price at $t = 0$ for several $\frac{h}{\sigma}$ values very near resonance. Note how the option moves to the left side of Fig. 14 and at the same time its value is attenuated when h approaches to resonance (with $h < \sigma$) and reappears on the right side of Fig. 14, increasing its value when h moves away from the resonance (with $h > \sigma$).

Figs. 15 and 16 show this behaviour by plotting the option price at $t = 0$ versus $\frac{h}{\sigma}$. Fig. 16 is a 180 degree view of Fig. 15. (See Figs. 15 and 16.)

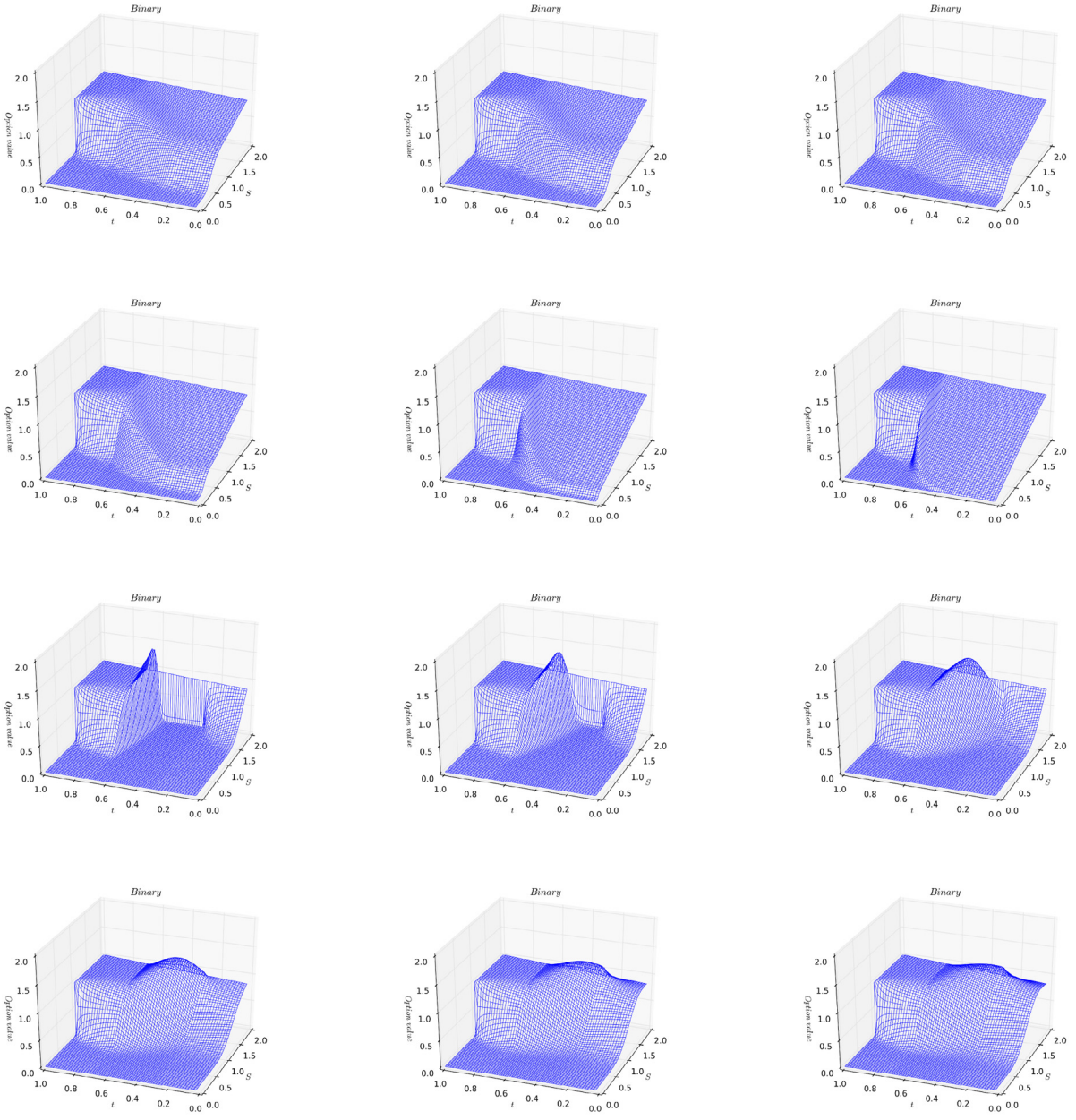

Fig. 12. From left to right and from top to bottom, European binary options for $\frac{h}{\sigma}$ = 0.90, 0.92, 0.94, 0.96, 0.98, 0.99, 1.01, 1.02, 1.04, 1.06, 1.08, 1.10 respectively.

9.2. Barrier binary options

Fig. 17 shows the results of the numerical integration of the B–S equation (11) under the action of the arbitrage bubble (14) in the case of a barrier binary option for several quotients $\frac{h}{\sigma}$, as indicated in Fig. 17. The parameters used are the same as in Fig. 11. Note that near the resonance but with $h < \sigma$, the propagator turns right and the same time decreases in value. For $h > \sigma$, the propagator turns left, dragging information of the middle sector of the option to the left. Now, the net result is that the option value at time $t = 0$ decreases to zero very near the resonance for both the left and right directions. (See Fig. 17.)

Fig. 18 shows the behaviour of the barrier binary option price at $t = 0$ for several values of $\frac{h}{\sigma}$ very near the resonance. Note how the option moves to the left side of Fig. 18 and at the same time its value is attenuated when h approaches the resonance (with $h < \sigma$) and reappears on the right side of Fig. 18 increasing its value when h moves away from the resonance (with $h > \sigma$).

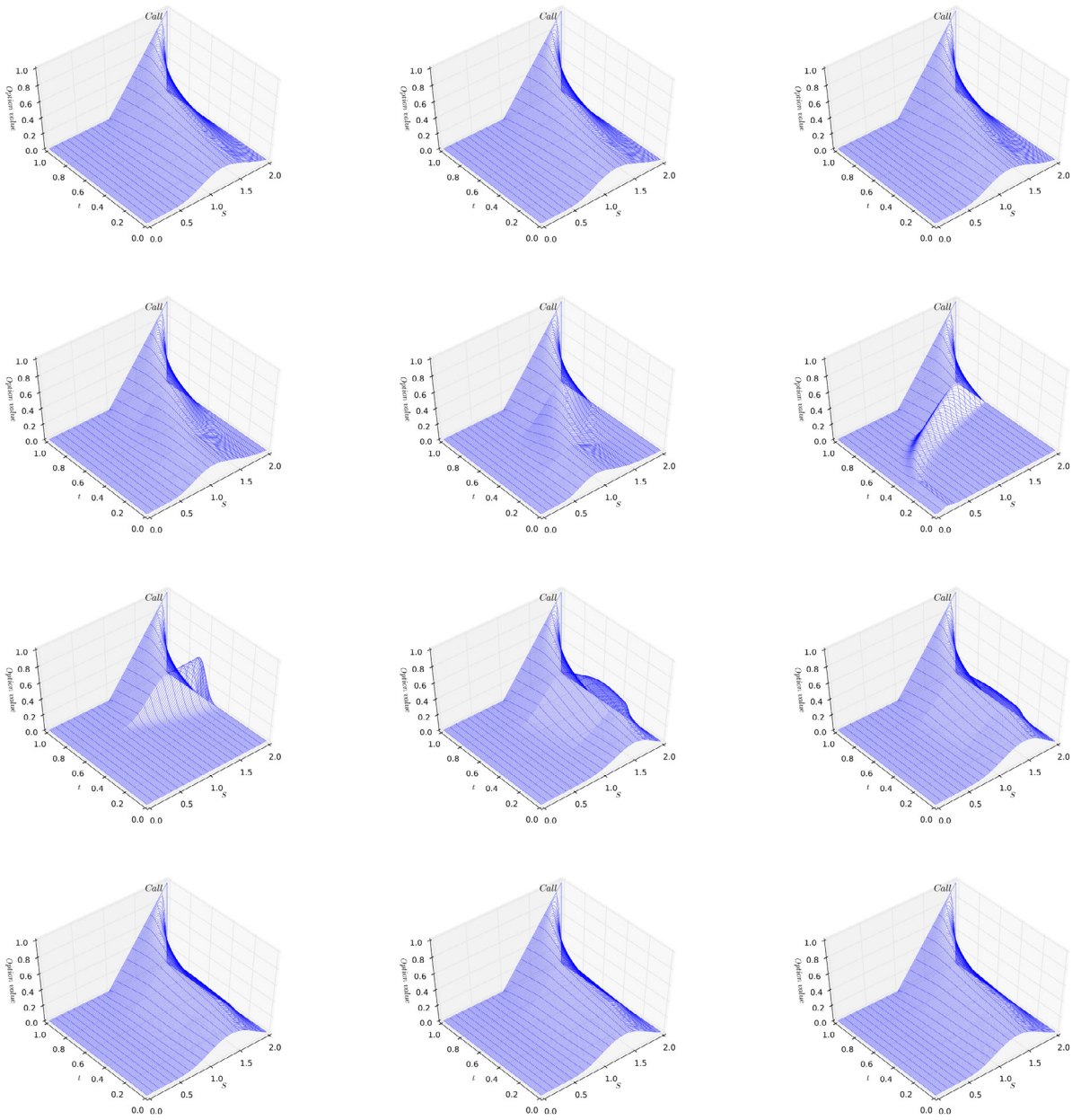

Fig. 13. From left to right and from top to bottom, barrier call options for $\frac{h}{\sigma}$ = 0.2, 0.4, 0.6, 0.8, 0.9, 0.98, 1.02, 1.1, 1.2, 1.4, 1.6, 1.8 respectively.

Figs. 19 and 20 show this behaviour by plotting the option price at $t = 0$ versus $\frac{h}{\sigma}$. Fig. 20 is a 180 degree view of Fig. 19. (See Figs. 19 and 20.)

10. Conclusions

In this article, we have analysed the price behaviour of options when the market is not perfect. These imperfections give rise to an arbitrage bubble that must be explicitly incorporated into the Black–Scholes equation as has been done in [27]. The net effect of the bubble is to generate a potential that completely changes the usual dynamics of the Black–Scholes model. On the basis of the empirical analysis carried out with real financial data in [27], the shape of this bubble is that of a function of the Heaviside type, which has a finite temporal duration and a characteristic amplitude which is a measure of the deviation from the (B–S) model produced by market imperfections. During the life of the option, the interest rate changes, and an effective rate is generated that depends on the bubble amplitude. When the bubble amplitude equals the

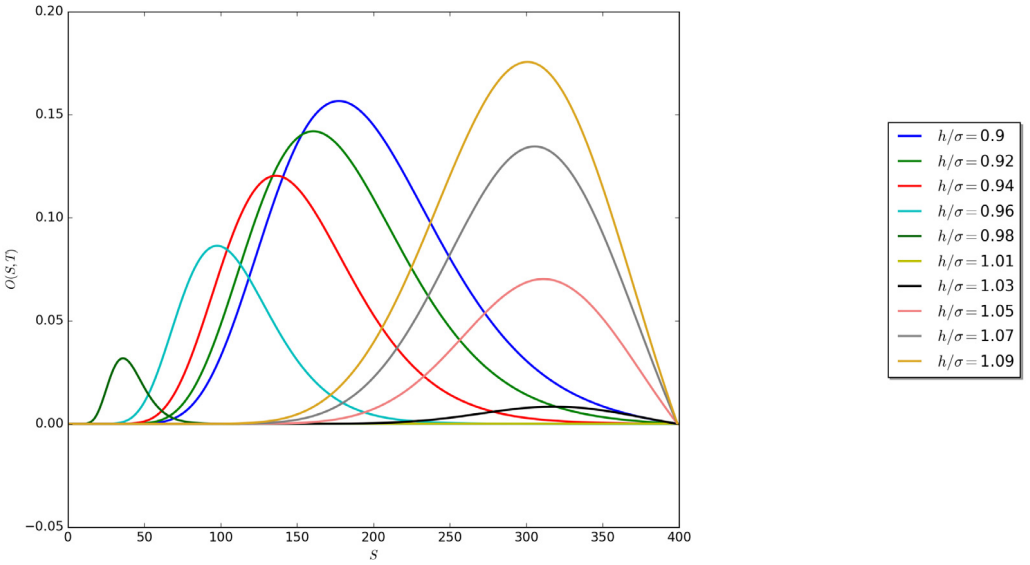

Fig. 14. Barrier call option value at $t = 0$, for several values of $\frac{h}{\sigma}$.

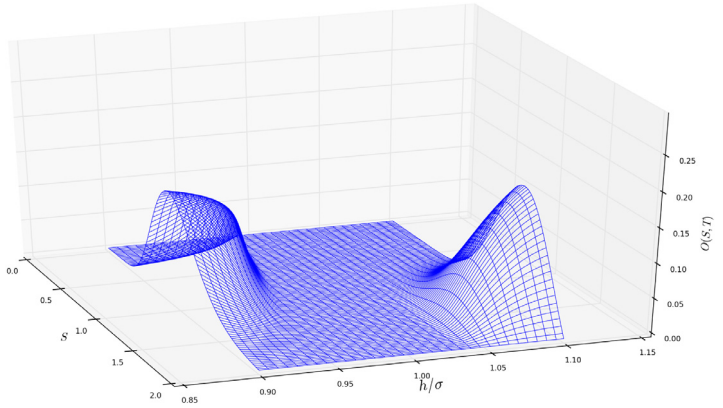

Fig. 15. Barrier call option value at $t = 0$ as a function of $\frac{h}{\sigma}$, view 1.

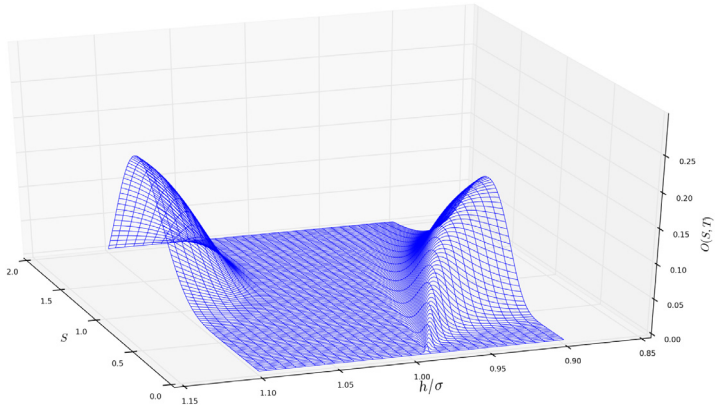

Fig. 16. Barrier call option value at $t = 0$ as a function of $\frac{h}{\sigma}$, view 2.

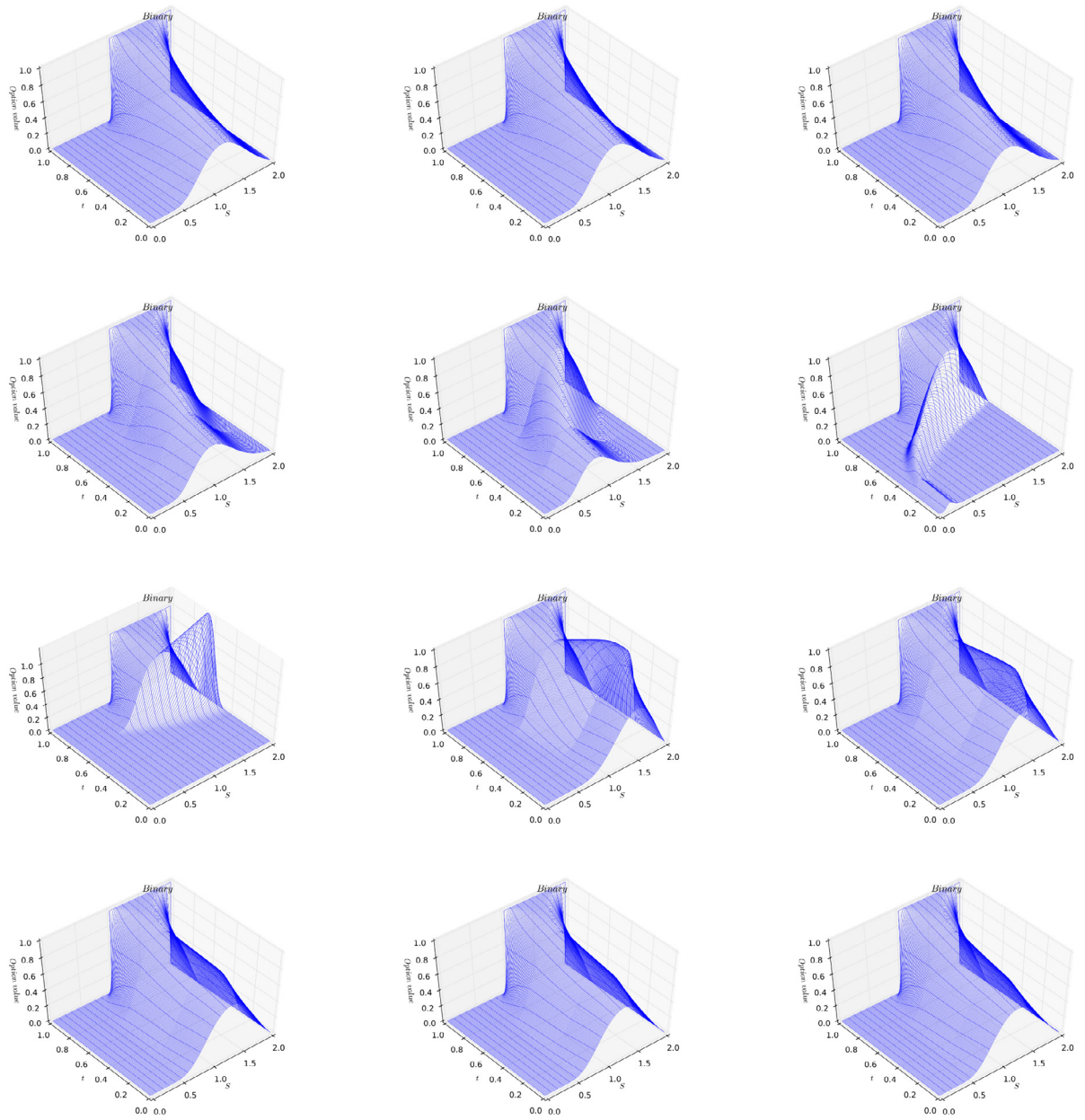

Fig. 17. From left to right and from top to bottom, barrier binary options for $\frac{h}{\sigma}$ = 0.2, 0.4, 0.6, 0.8, 0.9, 0.98, 1.02, 1.1, 1.2, 1.4, 1.6, 1.8 respectively.

market's volatility used in the B–S model, then both the potential and the effective interest rate become infinite, that is, a resonance occurs, analogously to what happens in mechanical or electrical systems. In order to determine what are its implications for the solution of the Black–Scholes equation, the behaviour of its propagator must be analysed. This has been done for both European and barrier options.

To study the propagator, a point of view similar to that of geometric optics was used, which is characterised by the analysis of light rays. In the financial case, the light rays associated with the propagator correspond to the trajectory of its maximum on the plane $(S - t)$. In this sense, the appearance of markets imperfections, that give rise to the arbitrage bubble, is equivalent to placing a glass or lens along the path of the light beam of the option propagator.

For a European option (when the effective interest rate is positive and very large), the light ray that comes from the time of maturity T turns right in the plane $(S - t)$ when it reaches the lens at time $t = T_2$, and at the same time, its value drops to zero. On the other hand, when the effective interest rate is very negative, the beam of the option doubles towards the left, and at the same time, the propagator's value grows. In the case of resonance, this effect occurs instantaneously

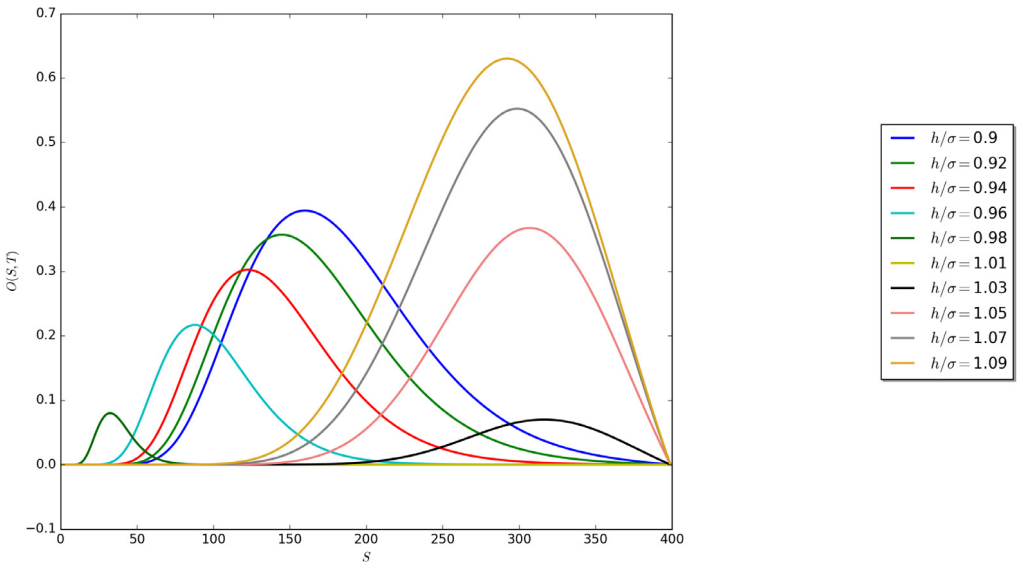

Fig. 18. Barrier binary option value at $t = 0$, for several values of $\frac{h}{\sigma}$.

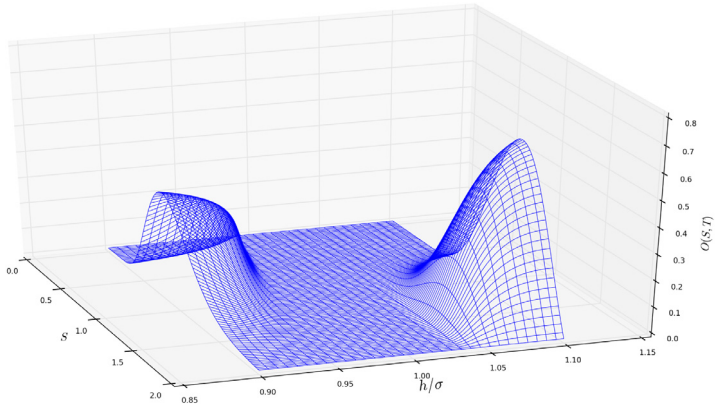

Fig. 19. Barrier binary option value at $t = 0$ as a function of $\frac{h}{\sigma}$, view 1.

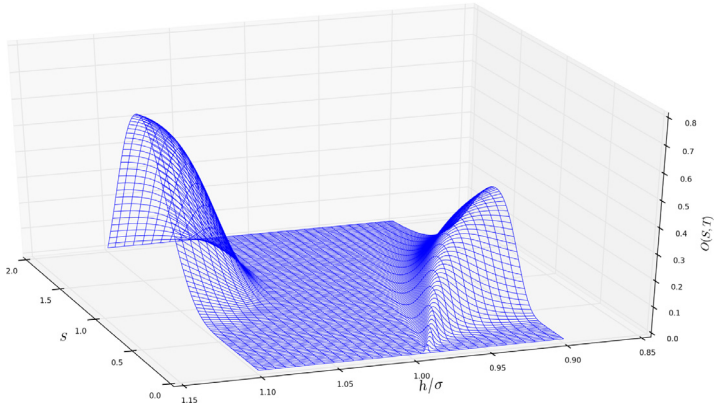

Fig. 20. Barrier binary option value at $t = 0$ as a function of $\frac{h}{\sigma}$, view 2.

and reminds one of the phenomena of total internal reflection in optics. Thus, for an observer located on the other side of the glass, the propagator's light ray is dimmed to the right or amplified to the left. In this case, its exact consequences for the option price depend on the option's boundary and initial conditions, because the option price is the convolution of the propagator with the contract function.

For a barrier option, the same effect occurs, but now the propagator's light beam is attenuated for both directions (left and right). Thus, due to this independence from the propagator's light ray direction, it is attenuated when it reaches the bubble, so the option price should decrease, and at the resonance, it should become zero.

We can conclude in this way that the usual Black–Scholes model corresponds, from the optics point of view to the situation in which light rays propagate freely in a vacuum without any interference. Market imperfections, then, can drastically change the dynamics of the option price, generating behaviour unexpected in the usual Black–Scholes model. When the resonance occurs, and the crystal of the arbitrage bubble deflects all the option's light rays, a crisis is generated in the financial system, causing untoward changes in the prices of options.

References

[1] F. Black, M. Scholes, The pricing of options and corporate liabilities, J. Political Econ. 8 (31) (1973) 637–654.
[2] R.C. Merton, Theory of rational option pricing, Bell J. Econ. Manage. Sci. 4 (1) (1973) 141–183.
[3] S. Heston, A closed form solution for option with stochastic volatility, with applications to bond and currency options, Rev. Financ. Stud. 6 (1993) 327–343.
[4] J. Hull, A. White, The pricing of options on assets with stochastic volatilities, J. Finance 42 (2) (1987).
[5] L. Chen, Stochastic mean and stochastic volatility: A three-factor model of the term structure of interest rates and its application to the pricing of interest rate derivatives, Financial Mark. Inst. Instrum. 5 (1996) 1–88.
[6] P. Wilmott, Paul Wilmott on Quantitative Finance, Wiley, 2000.
[7] J. Gatheral, The Volatility Surface, Wiley, 2006.
[8] B. Dupire, Pricing with a smile, Risk Mag. 7 (1994) 18–20.
[9] B. Dupire, Pricing and hedging with smiles, in: M. Dempster, S. Pliska (Eds.), Mathematics of Derivative Securities, Cambridge University Press, 1997.
[10] R. Cont, P. and Tankov, Financial Modelling with Jump Processes, Chapman and Hall, 2004.
[11] T. Björk, Arbitrage Theory in Continuous Time, third ed., Oxford, 2009.
[12] P.G. Zhang, Exotic Options, World Scientific, Singapore, 1997.
[13] B. Cornell, K. French, Taxes and the pricing of stock index futures, J. Finance 38 (3) (1983) 675–694.
[14] S. Figlewski, Hedging performance and basis risk in stock index futures, J. Finance 39 (3) (1984) 657.
[15] H.R. Stoll, R. Whaley, Program trading and expiration-day effects, Financ. Anal. J. 43 (2) (1987) 16–18+20–28.
[16] M. Brennan, E. Schwartz, Arbitrage in stock index futures, J. Bus. 63 (1) (1990) S7–S31.
[17] J. Liu, F. Longstaff, Losing money on arbitrage, Rev. Financ. Stud. 17 (3) (2003) 611–641.
[18] M. Attari, A. Mello, Financially constrained arbitrage in illiquid markets, J. Econom. Dynam. Control 30 (12) (2006) 2793–2822.
[19] T. Adrian, Inference, arbitrage, and asset price volatility, J. Financ. Intermediation 18 (1) (2009) 49–64.
[20] K. Ilinski, Physics of Finance: Gauge Modelling in Non–Equilibrium Pricing, Willey, 2001.
[21] K. Ilinski, How to Account for the Virtual Arbitrage in the StandArd Derivative Pricing, preprint.cond-mat/9902047, 1999, unpublished.
[22] K. Ilinski, A. Stepanenko, Derivative Pricing with Virtual Arbitrage, preprint.cond-mat/9902046, 1999, unpublished.
[23] M. Otto, Stochastic relaxational dynamics applied to finance: Towards non-equilibrium option pricing theory, Eur. Phys. J. B 14 (2) (2000) 383–394.
[24] S. Panayides, Arbitrage opportunities and their implications to derivative hedging, Physica A 361 (1) (2006) 289–296.
[25] S. Fedotov, S. Panayides, Stochastic arbitrage return and its implication for option pricing, Physica A 345 (2005) 207–217.
[26] G. Papanicolaou, K. Sircar, Stochastic volatility, smiles and asymptotics, Appl. Math. Finance 6 (1999) 107–145.
[27] M. Contreras, R. Montalva, R. Pellicer, M. Villena, Dynamic option pricing with endogenous stochastic arbitrage, Physica A 389 (17) (2010) 3552–3564.
[28] M. Contreras, R. Pellicer, D. Santiagos, M.Villena, Calibration and simulation of arbitrage effects in a non-equilibrium quantum black–scholes model by using semi-classical methods, J. Math. Finance 6 (2016) 541–561.
[29] M. Contreras, R. Pellicer, A. Ruiz, M. Villena, A quantum model of option pricing: When black–scholes meets Schrödinger and its semi-classical limit, Physica A 389 (23) (2010) 5447–5459.